JoP Journal of Pharmacopuncture

Journal of Pharmacopuncture 2025;28(1):57-68
pISSN: 2093-6966 • eISSN: 2234-6856
https://doi.org/10.3831/KPI.2025.28.1.57

Original Article

Bupleuri Radix Ameliorates Vascular Inflammation in Human Umbilical Vein Endothelial Cells via Modulation of Tight Junction Protein Expression and Inhibition of Nuclear Factor-κB Activation

Min Yeong Kim[1], Eun Jin Bang[1], Yung Hyun Choi[1,2], Su Hyun Hong[1,2]*

[1]Anti-Aging Research Center, Dong-Eui University, Busan, Republic of Korea
[2]Department of Biochemistry, Dong-Eui University College of Korean Medicine, Busan, Republic of Korea

Received December 23, 2024
Reviewed January 19, 2025
Accepted February 4, 2025

***Corresponding Author**
Su Hyun Hong
Department of Biochemistry, Dong-Eui University College of Korean Medicine, 52-57 Yangjeong-ro, Busanjin-gu, Busan 47227, Republic of Korea
Tel: +82-51-890-3334
E-mail: hongsh@deu.ac.kr

Objectives: The vascular endothelium plays a central role in the maintenance of vascular homeostasis. Inflammation of vascular endothelial cells has been closely related to the development of a wide range of cardiovascular diseases, including atherosclerosis. Bupleuri Radix (BR) possesses several biological properties, including anticancer, antimicrobial, antiviral, immunomodulatory, and anti-inflammatory properties. Furthermore, it can prevent and cure several diseases, such as the common cold, hepatitis, menoxenia, and hyperlipidemia. However, it is unclear whether BR can regulate vascular endothelial function under inflammatory conditions induced by interleukin-1β (IL-1β), a key proinflammatory cytokine. Therefore, in this study, we aimed to investigate the effect of BR on endothelial cell function using human umbilical vein endothelial cells (HUVECs) with IL-1β-induced inflammation.

Methods: The effects of BR on cell migration, angiogenesis, and monocyte adhesion were determined using scratch wound-healing assay, tube-formation assay, cell adhesion assay, fluorescein isothiocyanate-dextran Transwell assay, and transepithelial electrical resistance assay. The expression of tight junction (TJ) protein and adhesion molecules was estimated using western blotting and immunofluorescence assay. The generation of reactive oxygen species was assessed using flow cytometry.

Results: BR significantly suppressed the proliferation, migration, and tube-formation ability of IL-1β-stimulated HUVECs, and the expression of adhesion molecules, especially intracellular adhesion molecule-1. BR also regulated TJ protein expression, thereby restoring the transepithelial electrical resistance value to a level comparable to that of IL-1β-treated HUVECs. Moreover, BR decreased the production of intracellular reactive oxygen species and the nuclear translocation of the nuclear factor-kappa-B p65 subunit.

Conclusion: These findings revealed for the first time that BR prevents IL-1β-induced inflammation of blood vessel. Therefore, BR has the potential to protect the damage of vascular endothelial cells and prevent the progression of cardiovascular diseases.

Keywords: Bupleuri Radix, human umbilical vein endothelial cells, tight junction protein, nuclear factor-kappa-B, vascular inflammation

INTRODUCTION

Cardiovascular diseases (CVD) are associated with high morbidity and mortality rates worldwide [1]. The mortality rate is estimated to reach 2.36 million persons per year by 2030 [2]. The main pathogenesis of CVD is endothelial cell damage caused by inflammation [3, 4]. Hence, to prevent the development and progression of CVD, there is a need for new drugs

that can suppress endothelial cell inflammation, manage controllable prognostic factors, and alleviate endothelial cell damage.

Bupleuri Radix (BR) is obtained by drying the roots of *Bupleurum falcatum* Linne (belonging to the family Umbelliferae) [5]. BR has traditionally been used to harmonize the liver and stomach and to alleviate chest pressure and pain [6]. *In vitro* and *in vivo* studies have revealed that BR exhibits anti-inflammatory [7], antioxidant [8], antiobesity [9], and anticancer [10] properties. Consequently, it can be used as a therapeutic agent for various inflammatory diseases [11]. However, limited research has been conducted on the direct effects of BR on vascular inflammation and CVD. CVD are associated with chronic inflammatory conditions, such as atherosclerosis, and regulating these inflammatory responses is crucial for cardiovascular health. Therefore, further studies are warranted to explore the impact of the anti-inflammatory properties of BR on vascular inflammation and CVD.

Interleukin (IL)-1β-induced endothelial inflammation and dysfunction play key roles in the etiology of CVD by reducing vascular homeostasis [12]. Considering the anti-inflammatory effects of BR, this study assessed whether BR can alleviate endothelial cell dysfunction in human umbilical vein endothelial cells (HUVECs) with IL-1β-induced inflammation.

MATERIALS AND METHODS

1. Sample preparation

BR samples were purchased from Seogyeong Herbal Medicine Co., Ltd. (Busan, Republic of Korea). The samples were placed in 70% ethyl alcohol for subsequent ultrasonic extraction (Powersonic 405; Hwashin Technology Co., Ltd., Seoul, Republic of Korea). BR powder was dissolved in sterile distilled water and filtered using a Minister® syringe filter (0.2 μm; Sartorius AG, Weender Landstraß, Germany). The resulting solution was diluted to appropriate concentrations (0.25-2 μg/mL) for subsequent use.

2. Cell culture

HUVECs and human leukemia cells (U937 cells) were purchased from the American Type Culture Collection (Manassas, VA, USA). HUVECs were cultured in Vascular Endothelial Growth Factor (VEGF) Endothelial Medium (VascuLife VEGF LifeFactors Kit; Lifeline Cell Technology, Frederick, MD, USA). U937 cells were cultured in Roswell Park Memorial Institute Medium (RPMI-1640; Welgene, Daegu, Republic of Korea) containing 10% fetal bovine serum (FBS; Welgene) and 100 units/mL penicillin/streptomycin (P/S) at 37℃ under 5% CO_2 conditions.

3. Measurement of cell viability using the 3-(4,5-dimethylthiazol–2-yl)-2,5-diphenyltetrazolium bromide (MTT) assay

The cytotoxicity of BR was assessed using the MTT assay. In brief, the cells were treated with appropriate concentrations (0.25-2.00 μg/mL) of BR extract and cultured for 24 h. These cells were then treated with 0.5 mg/mL MTT solution (Invitrogen, Carlsbad, CA, USA) and incubated for 2 h to induce the reaction. Subsequently, the medium containing MTT was removed, and dimethyl sulfoxide (Sigma-Aldrich Chemical, St. Louis, MO, USA) was added to completely dissolve the formazan crystals produced by the reaction. The dissolved formazan was transferred to a 96-well plate at 200 μL/well. Subsequently, the absorbance was measured at 540 nm using a microplate reader (Beckman Coulter Inc., Brea, CA, USA). The cytotoxicity is expressed as a percentage based on the control.

4. Scratch wound healing assay

HUVECs were seeded in a six-well plate (4×10^5 cells/well) and cultured at 37℃ for 24 h. A scratch wound was created using a 200-μL tip, and the cells were then washed twice with phosphate-buffered saline (PBS). Following this, a medium without VascuLife VEGF LifeFactors was added. After pretreatment with BR for 1 h, the cells were treated with IL-1β extract for 24 h. Cell migration distance was quantified using a wound healing size tool (ImageJ software, v1.8.0; NIH, Bethesda, MD, USA).

5. Tube formation assay

HUVECs were seeded on Matrigel (BD Biosciences, San Jose, CA, USA). After 1 h, when cell adhesion could be observed, the cells were treated with BR extract for 1 h and then treated with IL-1β for 24 h. Subsequently, fluorescence staining was performed using calcein acetoxymethyl ester (Calcein-AM; Biotium Inc., Fremont, CA, USA). The suppression of

 https://doi.org/10.3831/KPI.2025.28.1.57

tube formation was assessed using a Carl Zeiss™ Axio Vert.A1 inverted microscope (Oberkochen, Germany) and an EVOS FL Auto 2 imaging system (Thermo Fisher Scientific, Waltham, MA, USA). Quantitative evaluation of tube formation was performed using the ImageJ Angiogenesis Analyzer tool on the Gilles Carpentier Research Web Site (http://image.bio.methods.free.fr).

6. Western blotting

Samples were prepared using the Bio-Rad Protein Assay Kit (Bio-Rad Laboratories, Hercules, CA, USA). Proteins were then separated and transferred onto a nitrocellulose membrane (Thermo Fisher Scientific). The membrane was incubated with specific primary antibodies, and the bands were enhanced for analysis using chemiluminescence reagents (Thermo Fisher Scientific). Antibodies were purchased from Santa Cruz Biotechnology, Inc. (Dallas, TX, USA), Cell Signaling Technology, Inc. (Beverly, MA, USA), Thermo Fisher Scientific, and Abcam (Cambridge, UK) (Table 1).

7. Immunofluorescence assay

The cells were fixed with methanol for 15 min at 4℃. Subsequently, the nuclear membrane was permeabilized using 0.2% Triton X-100. The cellular reaction was blocked by incubating the cells with 5% BSA/PBS-T for 1 h. After overnight treatment with primary antibodies (Table 2) at 4℃, the cells were incubated with a secondary antibody for 1 h at 25℃. The nucleus was stained with 4',6-diamidino-2-phenylindole (DAPI) and fixed by crystal mounting. Images were captured using a fluorescence microscope (EVOS FL Auto 2 imaging system; Thermo Fisher Scientific).

Table 1. List of primary antibodies used for western blotting

Protein	Host species	Catalog number	Company	Antibody dilution
Claudin-1	Rabbit	51-9000	Thermo Fisher Scientific	1:1000
Claudin-2	Rabbit	32-5600	Thermo Fisher Scientific	1:1000
Claudin-3	Rabbit	34-1700	Thermo Fisher Scientific	1:1000
Claudin-4	Mouse	32-9400	Thermo Fisher Scientific	1:1000
Claudin-5	Rabbit	34-1600	Thermo Fisher Scientific	1:1000
ICAM	Mouse	sc-8439	Santa Cruz	1:1000
Occludin	Rabbit	PA5-20755	Thermo Fisher Scientific	1:1000
VCAM	Mouse	sc-1316	Santa Cruz	1:1000
ZO-1	Mouse	ZO-1-1A12	Invitrogen	1:1000
ZO-2	Rabbit	2847s	Cell Signaling Technology	1:1000
ZO-3	Rabbit	36-4100	Thermo Fisher Scientific	1:1000
NFκB p65	Rabbit	6956P	Cell Signaling Technology	1:1000
IκB-α	Rabbit	sc-371	Santa Cruz	1:1000
lamin B	Goat	sc-6216	Santa Cruz	1:1000
β-actin	Mouse	BS6007M	Bioworld, Bloomington	1:25000

Table 2. List of primary antibodies used for the immunofluorescence assay

Protein	Host species	Catalog number	Company	Antibody dilution
Claudin-1	Rabbit	51-9000	Thermo Fisher Scientific	1:500
ICAM	Mouse	sc-8439	Santa Cruz	1:500
Occludin	Rabbit	PA5-20755	Thermo Fisher Scientific	1:500
ZO-2	Rabbit	2847s	Cell Signaling Technology	1:500
NFκB p65	Rabbit	6956P	Cell Signaling Technology	1:250

8. Cell adhesion assay

U937 cells (1.2×10^5 cells/well) were stained with DAPI for 15 min and seeded in wells containing HUVECs treated with IL-1β and BR for 12 h. Subsequently, the cells were washed thrice with the culture medium to remove any detached cells. Finally, the U937 cells adhering to HUVECs were observed using a Carl Zeiss™ Axio Vert.A1 inverted microscope (Oberkochen) and an EVOS FL Auto 2 imaging system (Thermo Fisher Scientific).

9. Fluorescein isothiocyanate (FITC)–dextran Transwell assay

HUVECs (1.5×10^4 cells/well) were seeded in Transwell® polycarbonate membrane well inserts (6.5-mm diameter, 0.4-μm pore size; Corning Inc., NY, USA) and allowed to stabilize for 24 h. The cells were pretreated with BR for 1 h and then treated with IL-1β for 24 h. Fresh medium was added to the lower chamber of the Transwell insert, and the medium in the upper chamber was replaced with medium containing FITC–dextran (Invitrogen Life Technologies); the samples were incubated in the dark for 30 min. The medium in the lower chamber was transferred into a 96-well plate at 200 μL/well. Fluorescence was then measured using an ELISA reader (BioTek) at an excitation wavelength of 490 nm and emission wavelength of 520 nm.

10. Transepithelial electrical resistance (TEER) assay

HUVECs (1.5×10^4 cells/well) were seeded in Transwell® polycarbonate membrane well inserts (6.5-mm diameter, 0.4-μm pore size; Corning Inc.) and allowed to stabilize for 24 h. The cells were pretreated with BR for 1 h and then treated with IL-1β for 24 h. Saturation in the chamber was reached after 72 h. TEER of the exposed cells was then measured using Epithelial Volt-Ohm Meter 2 (EVOM2; World Precision Instruments, Sarasota, FL, USA).

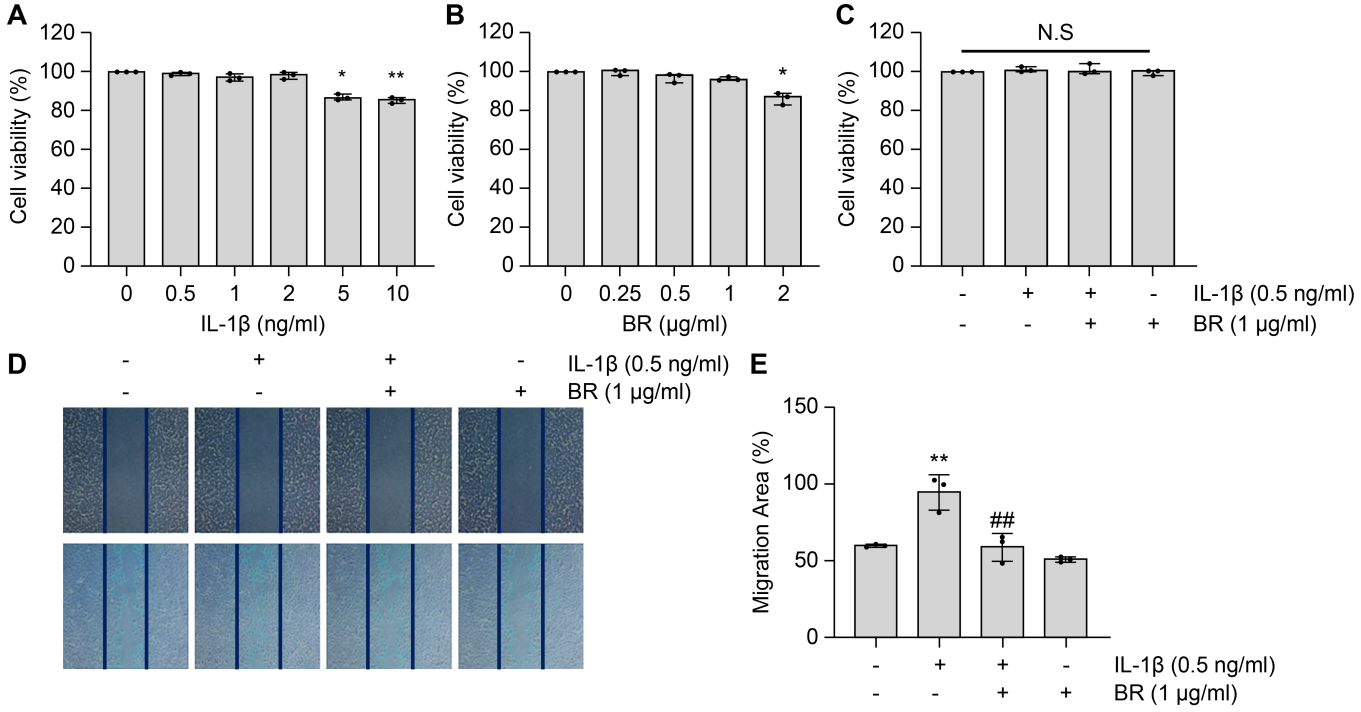

Figure 1. Effects of Bupleuri Radix (BR) on the viability and migration of interleukin-1β (IL-1β)-stimulated human umbilical vein endothelial cells (HUVECs). (A-C) HUVECs (2×10^5/mL) were seeded in six-well plates. The cells were treated with IL-1β and BR alone or together at the indicated concentrations. Cell viability was determined using the MTT assays. Values are expressed as mean ± SD (n = 3). (D) Cells were grown to confluence, and a wound was created in the cell layer using a 200 μL pipette tip. At the indicated time points, wound closure was observed under a microscope (×50), and images were captured. (E) Cell migration was calculated and expressed as the percentage of cell coverage to the initial cell-free zone. Differences between groups were determined using the ANOVA with Tukey's test (n = 3). *$p < 0.05$ and **$p < 0.01$ vs. control group; $^{\#\#}p < 0.01$ vs. IL-1β group.

 https://doi.org/10.3831/KPI.2025.28.1.57

11. Measurement of changes in reactive oxygen species (ROS) generation

The effect of BR on ROS generation after IL-1β treatment was determined by staining the cells with 2',7'-dichlorodihydrofluorescein diacetate (H2-DCF; Thermo Fisher Scientific). In brief, HUVECs were seeded in a 12-well plate (1.2×10^5 cells/well), cultured for 24 h, and then treated with 10 μM H2-DCF in a 5% CO_2 incubator at 37℃ for 20 min. The changes in ROS generation were measured using a BD Accuri C_6 flow cytometer (BD Biosciences). Moreover, the cells cultured under identical conditions were treated with H2-DCF in the dark for 20 min, washed twice with PBS, and then fixed with 3.7% paraformaldehyde. The fixed cells were again washed twice with PBS, and fluorescence intensity was assessed using EVOS FS Auto (Thermo Fisher Scientific). N-acetylcysteine (NAC) and mitoTEMPO were used as appositive controls to estimate ROS generation.

12. Extraction of nuclear proteins

The cells were pretreated with BR extract for 1 h and subsequently treated with IL-1β for 24 h. Then, they were harvested and centrifuged at 842 ×*g* for 5 min at 4℃. The nuclei and cytoplasm of the collected cells were isolated using the NE-PER Nuclear and Cytoplasmic Extraction Kit (Thermo Fisher Scientific). Proteins were quantified using Bio-Rad reagent (Bio-Rad Laboratories).

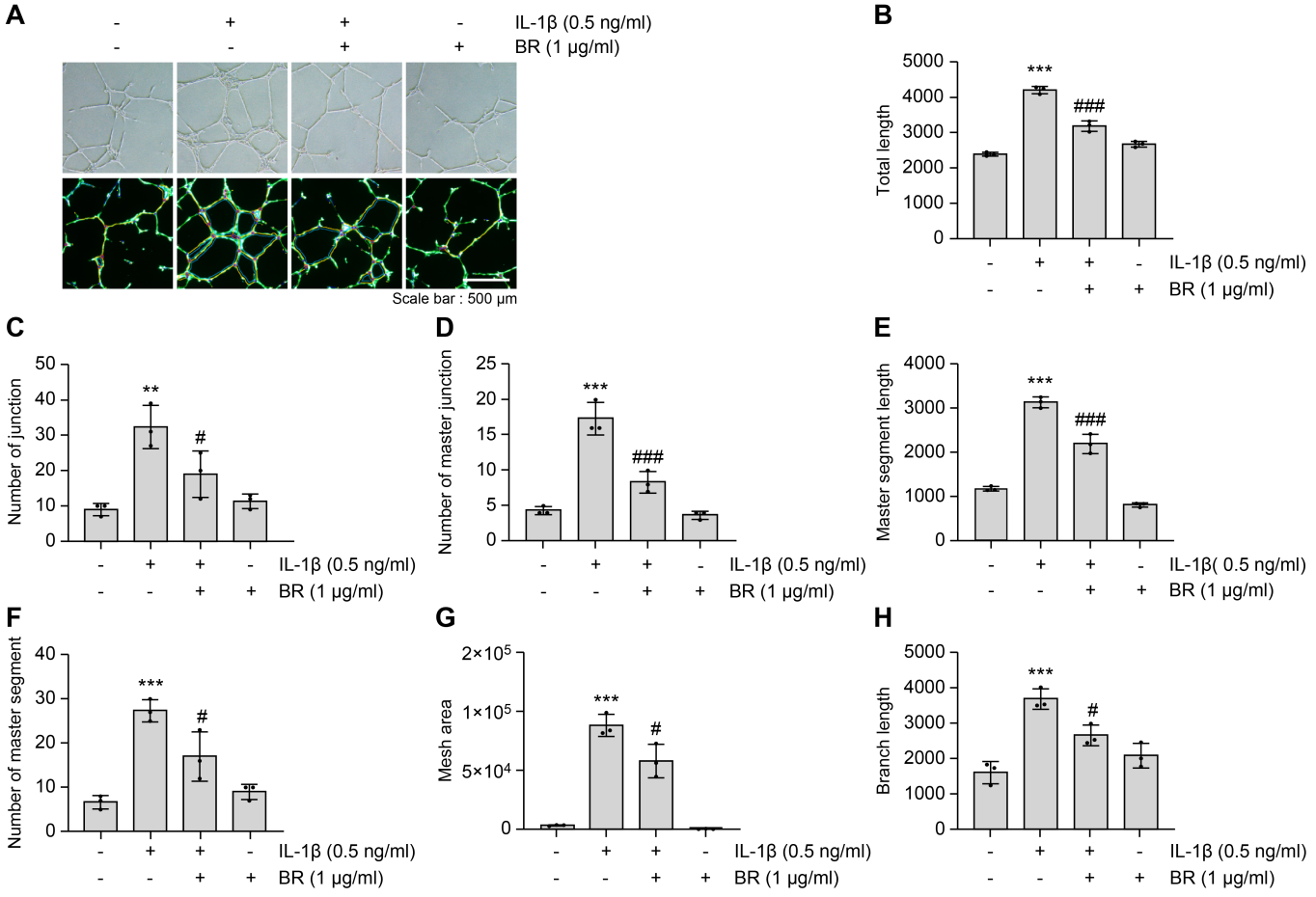

Figure 2. Effect of BR on the tube-formation ability of IL-1β-induced HUVECs. HUVECs were treated with BR (1 μg/mL) for 1 h, and then with IL-1β (10 ng/mL) for 24 h. Capillary tube formation (scale bar, 500 μm) (A), total length (B), number of junctions (C), number of master junctions (D), master segment length (E), number of master segments (F), mesh area (G), and branch length (H) of tubes per field were quantified by counting three random fields per well under a microscope. Values are expressed as mean ± standard deviation of three independent experiments. Differences between groups were determined using ANOVA with Tukey's test. $^{**}p < 0.01$, and $^{***}p < 0.001$ vs. control group; $^{\#}p < 0.05$ and $^{\#\#\#}p < 0.001$ vs. IL-1β group.

13. Network pharmacology analysis

The potential target genes involved in the association between BR and atherosclerosis were identified using the Traditional Chinese Medicine Integrative Database (TCMID) (https://bidd.group/TCMID) and DisGeNet (https://www.disgenet.org). In total, 53 BR target genes were further analyzed using the Java Enrichment of Pathways Extended To TOpology (JEPPETTO) plug-in for gene enrichment based on the Kyoto Encyclopedia of Genes and Genomes (KEGG) platform of Cytoscape (Ver. 3.9.1, https://cytoscape.orgβ). The potential target genes involved in the association between BR and atherosclerosis were used to analyze protein–protein interactions (PPIs) based on the STRING plug-in of Cytoscape.

14. Statistical analysis

Differences between groups were analyzed by one-way analysis of variance with Tukey's test using GraphPad Prism (version 8.4.2; GraphPad Software Inc., La Jolla, CA, USA). Statistical significance was set at $p < 0.05$.

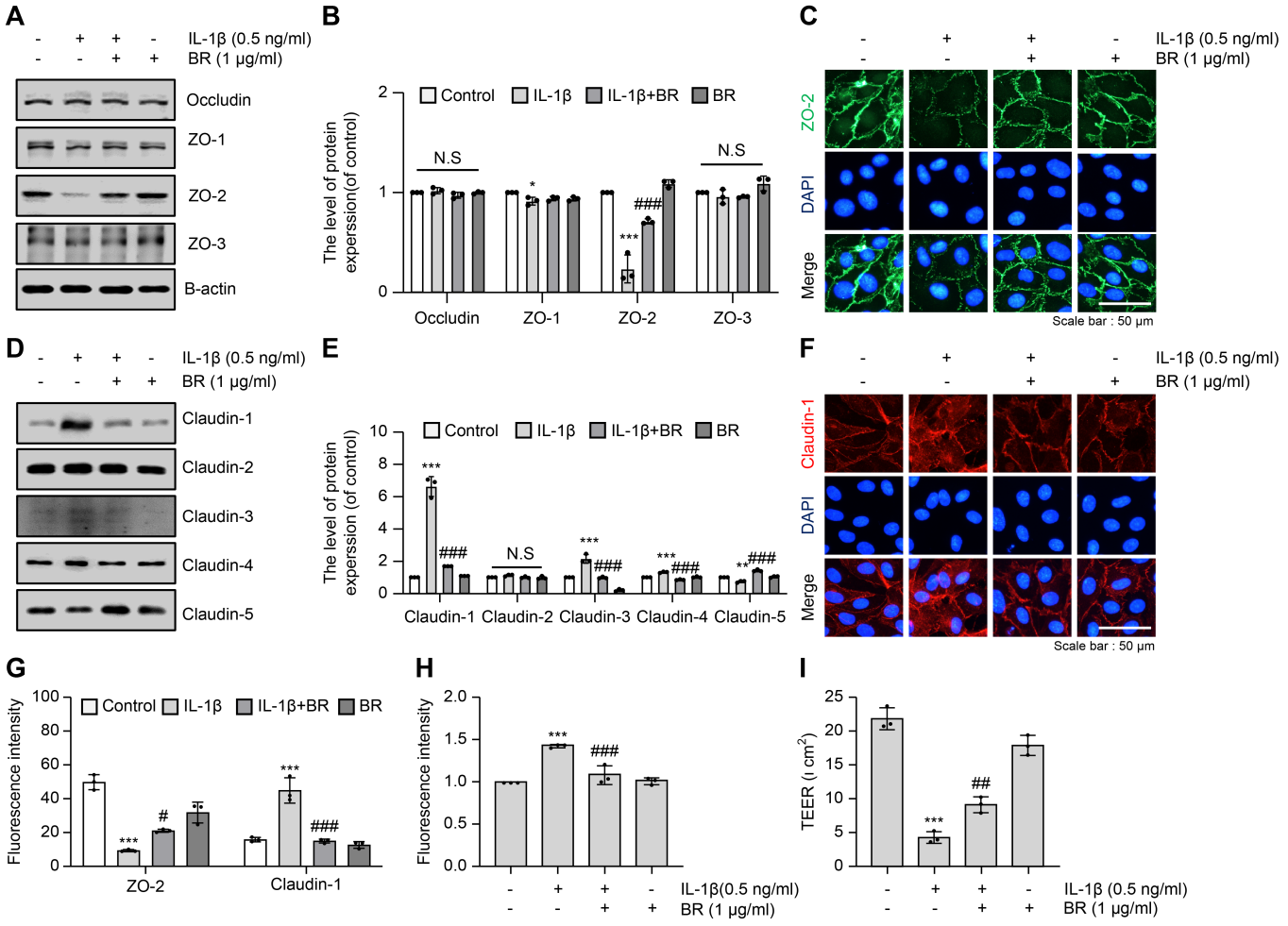

Figure 3. Effect of BR on the expression level of TJ-related proteins in IL-1β-induced HUVECs. (A, D) The cells were treated with BR for 1 h, and then with IL-1β for 24 h; Western blot analysis using specific antibodies was performed. (B, E) The quantification of (A) and (D), respectively. (C, F) Immunofluorescence staining for ZO-2 (green) and claudin-1 (red) was detected. Cell nuclei were stained blue with DAPI (blue). (G) Fluorescence intensity of ZO-2 (C) and claudin-1 (F) was analyzed. (H) FITC-dextran Transwell assay was carried out. (I) The TEER of the HUVEC monolayer was detected using EVOM2. Differences between groups were determined using ANOVA with Tukey's test (n = 3). *$p < 0.05$, **$p < 0.01$, and ***$p < 0.001$ vs. control group; $^{\#}p < 0.05$, $^{\#\#}p < 0.01$, and $^{\#\#\#}p < 0.001$ vs. IL-1β group.

 https://doi.org/10.3831/KPI.2025.28.1.57

RESULTS

1. BR suppresses cell migration and angiogenesis in IL-1β-stimulated HUVECs

Vascular cell inflammation increases cell migration and neovascularization [13]. In our study, BR inhibited the migration of IL-1β-stimulated HUVECs without inducing toxicity (Fig. 1). We performed a tube formation assay to determine whether BR could suppress angiogenesis in IL-1β-stimulated HUVECs. IL-1β treatment increased tube formation in HUVECs. However, BR pretreatment resulted in lower tube formation than IL-1β treatment alone (Fig. 2A). Analysis of neovascularization images using the Gilles Carpentier Research Web Site revealed markedly lower neovascularization (Fig. 2B-H) in cells pretreated with BR than in those treated with IL-1β alone.

2. BR regulates tight junction (TJ) protein expression and thereby restores cell barrier functions

Cell barrier defects caused by changes in tight junction (TJ) protein expression in the epithelium facilitate the onset of vascular inflammation that is associated with various diseases [14]. Therefore, we determined whether BR could regulate TJ protein expression in IL-1β-stimulated HUVECs. The expression level of zonula occludens (ZO)-2, a protein related to TJs, markedly decreased after 24 h of treatment with IL-1β; however, its level was restored to that in the control group in cells pretreated with BR for 1 h (Fig. 3A, B). Assessment of changes in ZO-2 expression using fluorescence staining yielded the same result (Fig. 3C, G). Among claudins, another group of proteins related to TJs, the expression level of only claudin-1 distinctly increased after IL-1β treatment. Western blotting and immunofluorescence staining revealed that the expression level decreased to the level in the control group after BR treatment (Fig. 3D-G). We also examined the changes in endothelial cell permeability after IL-1β and BR treatments by measuring the level of FITC–dextran (70 KD) infiltration through the HUVEC monolayer. The permeability of cells to FITC–dextran that had been increased by IL-1β treatment tended to decrease after BR pretreatment (Fig. 3H). Moreover, BR treatment restored the TEER level that had been markedly decreased by IL-1β treatment (Fig. 3I). These results indicate that BR regulates TJ protein expression altered during vascular inflammation, thereby contributing to the protection of vascular barrier functions.

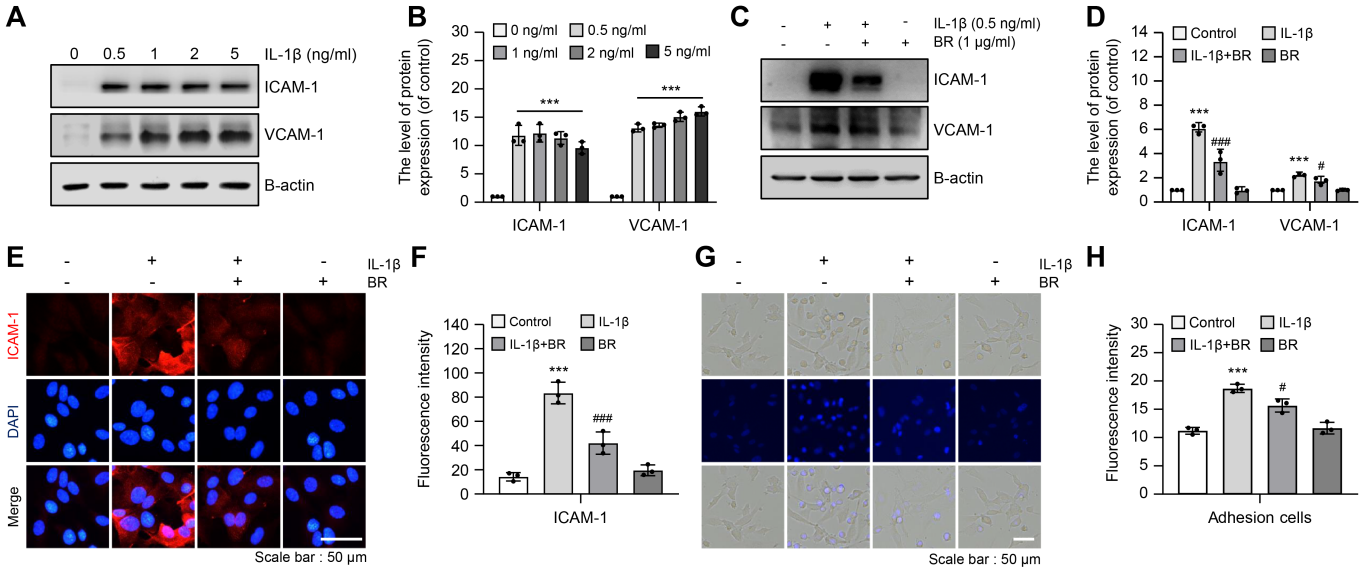

Figure 4. Effect of BR on the expression levels of adhesion molecules and adhesion of monocytes in IL-1β-stimulated HUVECs. Western blot analysis (A, C) and quantification (B, D) are shown. ICAM-1 and VCAM-1 expression was determined using immunofluorescence staining (E, F), and the fluorescence intensity was quantified. (G) U937 monocyte adhesion to HUVECs was evaluated using a cell adhesion assay. (H) Fluorescence intensity in 4D was analyzed in three random fields under a microscope. Values are expressed as mean ± standard deviation of three independent experiments. Differences between groups were determined using ANOVA with Tukey's test. ***$p < 0.001$ vs. control group; $^{\#}p < 0.05$ and $^{\#\#\#}p < 0.001$ vs. IL-1β group.

3. BR lowers adhesive molecule expression, monocyte adhesion, and cell permeability

Under inflammatory conditions, the expression levels of adhesive molecules, such as ICAM-1 and VCAM-1, increase. Moreover, the migration of monocytes in vascular endothelial cells is enhanced [15]. Therefore, we examined the changes in the expression levels of ICAM-1 and VCAM-1 in IL-1β-stimulated HUVECs. As shown in Fig. 4A and B, the expression levels of ICAM-1 and VCAM-1 markedly increased in HUVECs after 24 h of treatment with IL-1β. However, the expression levels decreased after pretreatment with BR for 1 h (Fig. 4C, D). Furthermore, the immunofluorescence assay for ICAM-1, which showed a marked decrease in expression following BR treatment, revealed expression patterns identical to those observed in western blotting (Fig. 4E, F). Next, we performed an adhesion assay to evaluate the migration of white blood cells to vascular endothelial cells. As shown in Fig. 4G and H, the adhesion of U937 cells to HUVECs was markedly lower in the group pretreated with BR than in that treated with only IL-1β. These results indicate that BR downregulates the expression of adhesive molecules and reduces monocyte migration to suppress vascular inflammation.

4. BR reduces intracellular ROS generation

ROS are closely associated with various inflammatory diseases, including CVD [16]. Therefore, we assessed whether BR could control IL-1β-induced ROS generation in HUVECs. As shown in Fig. 5A and B, BR treatment markedly reduced the level of ROS generation in IL-1β-stimulated HUVECs. NAC (a ROS scavenger) and mitoTEMPO (a mitochondrial superoxide dismutase mimetic and peroxyl scavenger) were used as positive controls [17]. The antioxidant effect in BR-treated cells was

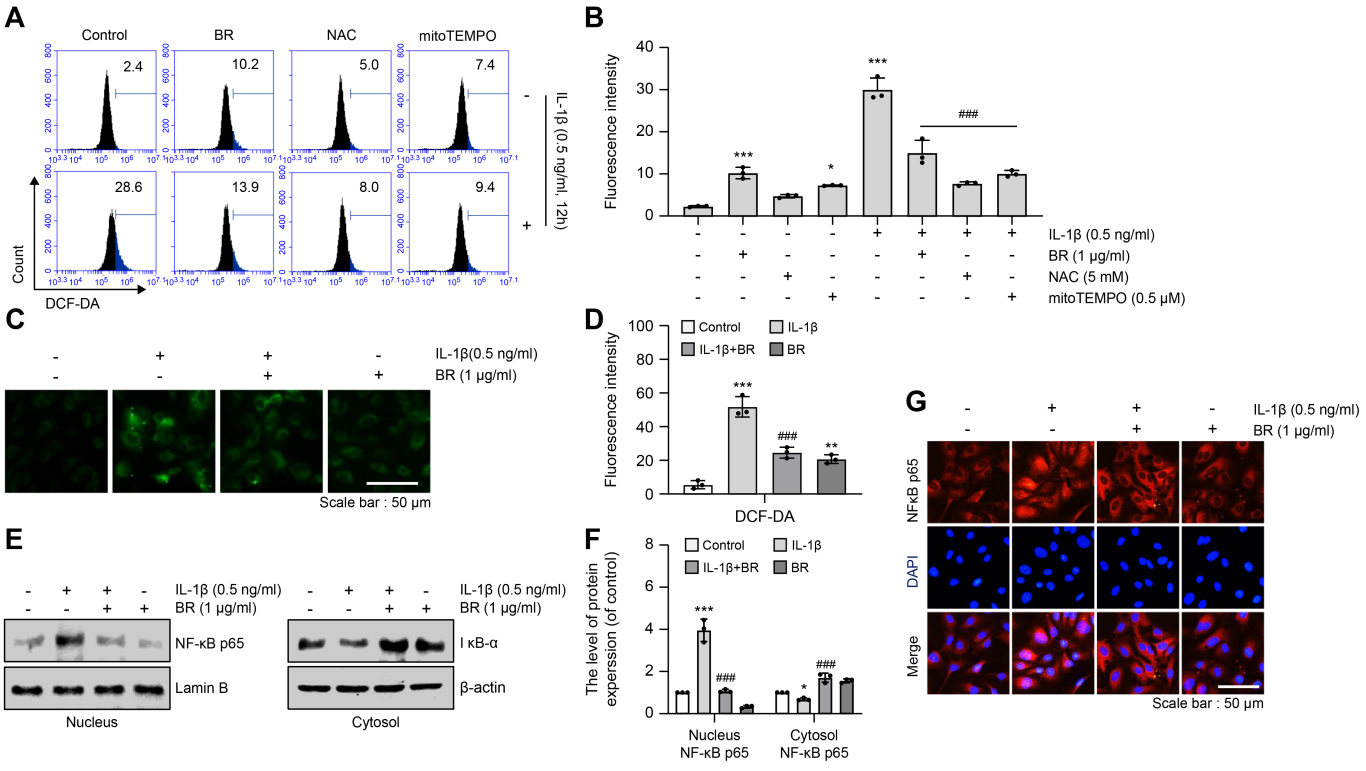

Figure 5. Effect of BR on the generation of ROS and nuclear translocation of NF-κB in IL-1β-stimulated HUVECs. (A) HUVECs were pretreated with BR, NAC, and mitoTEMPO for 1 h, and then treated with IL-1β for 12 h. The cells were stained with 10 μM H_2DCF-DA and analyzed using a flow cytometer. (B) The fluorescence intensity was quantified. Morphological changes in the stained cells were observed using a fluorescence microscope (C) and quantified (D). The protein levels of IκBα in the cytosolic fraction and p65 in the nuclear fraction were determined using western blot analysis (E) and quantified (F). (G) Cells were treated with 1 μg/mL BR for 1 h, and then with IL-1β for 24 h; subsequently, the cells were immunofluorescence stained with anti-NF-κB/p65 antibody (red) and visualized using a fluorescence microscope. Cell nuclei were stained with DAPI (blue). *p < 0.05, **p < 0.01, and ***p < 0.001 vs. control group; $^{###}$p < 0.001 vs. IL-1β group.

 https://doi.org/10.3831/KPI.2025.28.1.57

similar to that in the positive controls. Assessment of DCF-DA-stained cells under a fluorescence microscope revealed that the ROS levels that had increased after IL-1β treatment decreased after BR treatment (Fig. 5C, D). These results indicate that BR significantly reduces IL-1β-induced oxidative stress.

5. BR exhibits anti-inflammatory effects via nuclear factor kappa B (NF-κB) signal activation in IL-1-stimulated HUVECs

NF-κB is an important transcription factor that regulates the expression of proteins associated with inflammation [18]. As shown in Fig. 5E and F, the nuclear translocation level of the p65 subunit of NF-κB that had been increased after 24 h of treatment with IL-1β was restored to the level in the control group after 1 h of pretreatment with BR. Moreover, the cytoplasmic expression of NF-κB inhibitor α (IκB-α) that had been decreased after IL-1β treatment increased after BR treatment. The immunofluorescence assay also revealed the same trend (Fig. 5G). These results indicate that BR inhibits IL-1β-induced NF-κB activation, suppressing vascular inflammation.

6. Network pharmacology analysis predicts potential therapeutic effects of BR on atherosclerosis

We performed a network pharmacology analysis to further investigate the potential of BR as a preventive and therapeutic agent for atherosclerosis and to elucidate the underlying mechanisms. We generated a list of BR target genes using TCMID. We used these BR target genes in the network analysis with the JEPPETTO plug-in of Cytoscape to assess the correlation between genetic and biological functions. This KEGG-based gene enrichment analysis revealed that the peroxisome proliferator-activated receptor (PPAR) signaling pathway was most significantly related to the BR target genes (Fig. 6A). Moreover, steroid hormone biosynthesis, galactose metabolism, glycerol lipid metabolism, VEGF signaling, and arachidonic acid metabolism were correlated with cellular and pathological changes related to atherosclerosis. Furthermore, we verified whether BR could target the genes associated with atherosclerosis listed in DisGeNet. Based on the results, we identified 17 genes as shared target genes for BR and endometriosis (Fig. 6B). All genes, except for *F10*, exhibited strong PPIs (Fig. 6C).

DISCUSSION

In this study, we used HUVECs with IL-1β-induced inflammation to assess the preventive and therapeutic effects of BR. *In vitro* analyses revealed that BR can effectively suppress endothelial inflammation (Fig. 7). Inflammatory cytokines and excessive ROS activate vascular endothelial cells; this is the main cause of endothelial abnormalities that result in ischemic heart

A

Signaling pathway	XD-Score	q-value
PPAR signaling pathway	0.383	0.001
Steroid hormone biosynthesis	0.239	0.633
Galactose metabolism	0.208	0.633
Glycerolipid metabolism	0.172	0.698
VEGF signaling pathway	0.166	0.096
Arachidonic acid metabolism	0.126	0.804

B

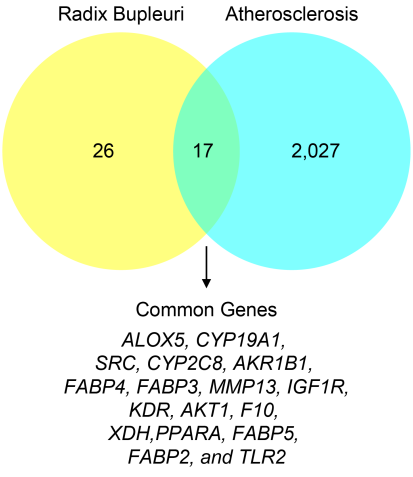

C

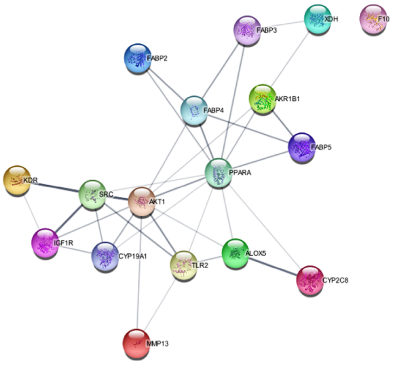

Figure 6. Potential therapeutic effect of Bupleuri Radix (BR) on atherosclerosis as predicted using a network pharmacological analysis. The Traditional Chinese Medicine Integrative Database and DisGeNet database were used to identify potential target genes for BR and atherosclerosis, respectively. (A) Potential signaling pathways of common target genes of BR and atherosclerosis were analyzed using the KEGG Pathway database with the JEPPETO plug-in in Cytoscape. (B) Shared genes between BR and atherosclerosis were compiled and presented using Venn diagram analysis. (C) Protein-protein interaction network of common genes was analyzed using the STRING plug-in in Cytoscape.

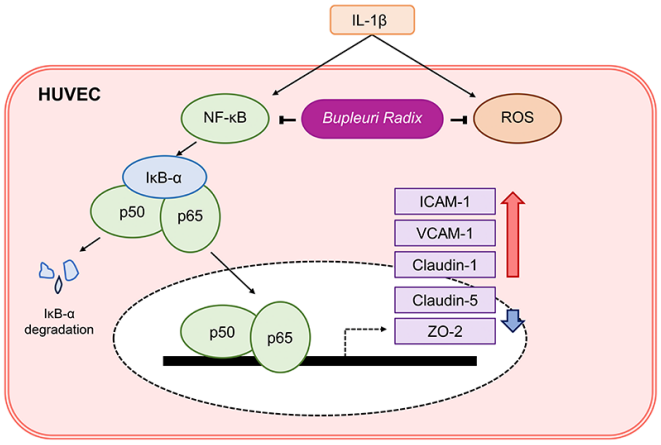

Figure 7. Schematic illustration of the study's findings.

diseases, such as myocardial infarction and stroke [19].

IL-1 is a representative proinflammatory cytokine similar to tumor necrosis factor (TNF). The IL-1 family consists of 11 distinct members. Of these, IL-1β exhibits major biological activities [20]. It induces the expression of E-selectin in vascular endothelial cells. Moreover, it increases the expression levels of adhesive molecules, such as ICAM-1 and VCAM-1, and integrin ligands in white blood cells, thereby promoting the adhesion of white blood cells and vascular endothelial cells [12, 21]. ICAM-1 is expressed in the early stages of atherosclerosis, whereas VCAM-1 is expressed in the late stages [22]. Consistently, ICAM-1 expression markedly increased within 30 min of IL-1 treatment in our study. Previous studies have revealed that the expression levels of ICAM-1 and VCAM-1 are closely associated with angiogenesis [22, 23]. In this study, IL-1β-stimulated HUVECs exhibited a marked increase in cross-linkages and connections with endothelial cells, along with increased expression levels of ICAM-1 and VCAM-1. Such angiogenesis-related processes were suppressed by BR treatment, suggesting the ability of BR to control vascular inflammation.

Vascular endothelial cells exhibit strong cell–cell binding to ensure response to blood flow and inflammatory reactions. The cell–cell connections that play a crucial role in the maintenance of the endothelial cell barrier include TJs, adherens junctions, and gap junctions. The TJ family includes ZO-1, ZO-2, and ZO-3, which are connected to the cytoplasm via occludins and claudins in the cell membrane [24]. Ni et al. [25] and Clark et al. [26] reported that claudin-5 and occludins play important roles in TJ formation in endothelial cells. In this study, IL-1β-stimulated HUVECs exhibited significantly altered expression of ZO-2, claudin-1, and claudin-5 after BR treatment. As BR contains various components, it is challenging to interpret the exact effect of specific components. Future studies should therefore assess the specific effect of BR components on cell barrier integrity. In this study, we demonstrated that BR maintains the integrity of vascular endothelial cells by regulating TJ expression *in vitro*. Our results indicate the protective effect of BR on endothelial cells during the inflammatory response.

Previous empirical studies on endothelial cell dysfunction induced by oxidative stress, TNF-α, LPS, or diabetes have revealed the key role of the activation of the NF-κB pathway [27-29]. NF-κB signaling for transcriptional activation occurs via classical (canonical) and alternative (noncanonical) pathways; both these pathways involve the dimerization of five proteins [p50, p52, p65 (RelA), RelB, and c-Rel] that bind with DNA to induce the expression of target proteins [20]. The canonical pathway is activated in most cases involving IL-1β stimulation. In particular, IκB-α is phosphorylated for degradation, and a dimer of p65 is translocated to the nucleus [30, 31]. Consistent with these reports, in our study, IL-1β treatment led to the activation of the canonical pathway and the nuclear translocation of a dimer of NF-κB p65. This phenomenon may regulate the expression of adhesive molecules (e.g., ICAM-1 and VCAM-1) and TJs (e.g., ZO-2, claudin-1, and claudin-5).

BR contains saikosaponins, volatile oils, polysaccharides, fatty acids, and sterols. Of these, saikosaponins serve as the most important physiologically active component [32]. In particular, saikosaponin a exhibits a strong anti-inflammatory effect and can alleviate the inflammatory response by regulating the NF-κB pathway and inhibiting ROS generation [33]. Further mechanistic studies are warranted to assess the protective effect of BR on vascular inflammation. Nevertheless, our results indicate that NF-kB may be an important mediator of the anti-inflammatory effects of BR.

Interestingly, we predicted the potential therapeutic effects of BR based on a network pharmacology analysis. We analyzed potential target genes obtained from TCMID and found that several signaling pathways, including PPAR signaling pathways, were associated with BR (Fig. 6). To confirm whether BR can effectively prevent arteriosclerosis, it is necessary to establish an animal model and assess the expression of related proteins and the underlying mechanisms in future research.

CONCLUSION

We investigated the protective effects of BR against vascu-

 https://doi.org/10.3831/KPI.2025.28.1.57

lar inflammation and elucidated the underlying mechanisms. BR reduced cell migration, suppressed angiogenesis, and decreased adhesive molecule expression, preventing the adhesion of monocytes to endothelial cells in IL-1β-stimulated HUVECs. Furthermore, BR maintained the integrity of vascular endothelial cells by regulating TJs through the suppression of intracellular ROS generation and nuclear translocation of NF-κB p65. Although further studies are warranted to validate the clinical efficacy of BR in suppressing vascular inflammation and maintaining TJ integrity and to elucidate the underlying mechanisms, our findings suggest that BR protects against inflammation-induced vascular injury and could help prevent CVD.

ACKNOWLEDGEMENTS

The authors would like to thank Editage (www.editage.co.kr) for English language editing.

AUTHORS' CONTRIBUTIONS

Conceptualization, MYK and SHH; Formal analysis and investigation, MYK and EJB; Data curation, SHH and YHC; Manuscript writing, MYK, EJB, and SHH; Review and edition; SHH; Visualization, MYK and YHC; Supervision, SHH; Funding acquisition, SHH. All authors have read and agreed to the published version of the manuscript.

ETHICAL APPROVAL

No ethical approval was required as this study did not involve human participants or laboratory animals. All procedures were carried out in adherence to the ethical principles outlined in the Declaration of Helsinki, as adopted by the World Medical Association.

DATA AVAILABILITY

The data that support the findings of this study are available within the article.

CONFLICTS OF INTEREST

The authors declare that they have no conflicts of interest.

FUNDING

This research was supported by the National Research Foundation of Korea (NRF) grant funded by the Korean Government (MSIT) (grant number 2022R1A2C1003573). The funders had no role in the design of study; collection, analysis and interpretation of data; writing of the report; and decision to submit the article for publication.

ORCID

Min Yeong Kim, https://orcid.org/0000-0001-9083-8218
Eun Jin Bang, https://orcid.org/0000-0003-3847-4992
Yung Hyun Choi, https://orcid.org/0000-0002-1454-3124
Su Hyun Hong, https://orcid.org/0000-0001-9291-5803

REFERENCES

1. Li Y, Cao GY, Jing WZ, Liu J, Liu M. Global trends and regional differences in incidence and mortality of cardiovascular disease, 1990-2019: findings from 2019 Global Burden of Disease Study. Eur J Prev Cardiol. 2023;30(3):276-86.
2. Kim MJ, Kang HH, Seo YJ, Kim KM, Kim YJ, Jung SK. *Paeonia lactiflora* root extract and its components reduce biomarkers of early atherosclerosis via anti-inflammatory and antioxidant effects in vitro and in vivo. Antioxidants (Basel). 2021;10(10):1507.
3. North BJ, Sinclair DA. The intersection between aging and cardiovascular disease. Circ Res. 2012;110(8):1097-108.
4. Goldsborough E 3rd, Osuji N, Blaha MJ. Assessment of cardiovascular disease risk: a 2022 update. Endocrinol Metab Clin North Am. 2022;51(3):483-509.
5. Do HJ, Kim K, Oh TW. Anti-hyperlipidemic effects of Scutellariae Radix, Aucklandiae Radix and Bupleuri Radix (SAB) extract in FL83B cells. Kor J Herbol. 2020;35(5):23-31.
6. Yang F, Dong X, Yin X, Wang W, You L, Ni J. *Radix Bupleuri*: a review of traditional uses, botany, phytochemistry, pharmacology, and toxicology. Biomed Res Int. 2017;2017:7597596.
7. Shen X, Zhao Z, Wang H, Guo Z, Hu B, Zhang G. Elucidation of the anti-inflammatory mechanisms of Bupleuri and Scutellariae Radix using system pharmacological analyses. Mediators Inflamm. 2017;2017:3709874.
8. Bak SB, Song YR, Bae SJ, Lee WY, Kim YW. Integrative approach to uncover antioxidant properties of Bupleuri Radix and its active compounds: multiscale interactome-level analysis with experimental validation. Free Radic Biol Med. 2023;199:141-53.
9. Wu L, Yan Q, Chen F, Cao C, Wang S. Bupleuri radix extract ameliorates impaired lipid metabolism in high-fat diet-induced

obese mice via gut microbia-mediated regulation of FGF21 signaling pathway. Biomed Pharmacother. 2021;135:111187.
10. Zhang F, Zhou K, Yuan W, Sun K. Radix Bupleuri-Radix Paeoniae Alba inhibits the development of hepatocellular carcinoma through activation of the PTEN/PD-L1 axis within the immune microenvironment. Nutr Cancer. 2024;76(1):63-79.
11. Jia R, Gu Z, He Q, Du J, Cao L, Jeney G, et al. Anti-oxidative, anti-inflammatory and hepatoprotective effects of Radix Bupleuri extract against oxidative damage in tilapia (Oreochromis niloticus) via Nrf2 and TLRs signaling pathway. Fish Shellfish Immunol. 2019;93:395-405.
12. Gan J, Guo L, Zhang X, Yu Q, Yang Q, Zhang Y, et al. Anti-inflammatory therapy of atherosclerosis: focusing on IKKβ. J Inflamm (Lond). 2023;20(1):8.
13. Chen CC, Li HY, Leu YL, Chen YJ, Wang CJ, Wang SH. Corylin inhibits vascular cell inflammation, proliferation and migration and reduces atherosclerosis in ApoE-deficient mice. Antioxidants (Basel). 2020;9(4):275.
14. Rawat M, Nighot M, Al-Sadi R, Gupta Y, Viszwapriya D, Yochum G, et al. IL1B increases intestinal tight junction permeability by up-regulation of MIR200C-3p, which degrades occludin mRNA. Gastroenterology. 2020;159(4):1375-89.
15. Videm V, Albrigtsen M. Soluble ICAM-1 and VCAM-1 as markers of endothelial activation. Scand J Immunol. 2008;67(5):523-31.
16. Park C, Cha HJ, Hwangbo H, Bang E, Hong SH, Song KS, et al. β-Asarone alleviates high-glucose-induced oxidative damage via inhibition of ROS generation and inactivation of the NF-κB/NLRP3 inflammasome pathway in human retinal pigment epithelial cells. Antioxidants (Basel). 2023;12(7):1410.
17. Janbandhu V, Tallapragada V, Patrick R, Li Y, Abeygunawardena D, Humphreys DT, et al. Hif-1a suppresses ROS-induced proliferation of cardiac fibroblasts following myocardial infarction. Cell Stem Cell. 2022;29(2):281-97.e12.
18. Zhong Y, He S, Huang K, Liang M. Neferine suppresses vascular endothelial inflammation by inhibiting the NF-κB signaling pathway. Arch Biochem Biophys. 2020;696:108595.
19. Chistiakov DA, Orekhov AN, Bobryshev YV. Endothelial barrier and its abnormalities in cardiovascular disease. Front Physiol. 2015;6:365.
20. Kaminsky LW, Al-Sadi R, Ma TY. IL-1β and the intestinal epithelial tight junction barrier. Front Immunol. 2021;12:767456.
21. Chen T, Zhang X, Zhu G, Liu H, Chen J, Wang Y, et al. Quercetin inhibits TNF-α induced HUVECs apoptosis and inflammation via downregulating NF-kB and AP-1 signaling pathway in vitro. Medicine (Baltimore). 2020;99(38):e22241.
22. Zhu Y, Xian X, Wang Z, Bi Y, Chen Q, Han X, et al. Research progress on the relationship between atherosclerosis and inflammation. Biomolecules. 2018;8(3):80.
23. Fotis L, Agrogiannis G, Vlachos IS, Pantopoulou A, Margoni A, Kostaki M, et al. Intercellular adhesion molecule (ICAM)-1 and vascular cell adhesion molecule (VCAM)-1 at the early stages of atherosclerosis in a rat model. In Vivo. 2012;26(2):243-50.
24. Wautier JL, Wautier MP. Vascular permeability in diseases. Int J Mol Sci. 2022;23(7):3645.
25. Ni Y, Teng T, Li R, Simonyi A, Sun GY, Lee JC. TNFα alters occludin and cerebral endothelial permeability: role of p38MAPK. PLoS One. 2017;12(2):e0170346.
26. Clark PR, Kim RK, Pober JS, Kluger MS. Tumor necrosis factor disrupts claudin-5 endothelial tight junction barriers in two distinct NF-κB-dependent phases. PLoS One. 2015;10(3):e0120075.
27. Pan W, Yu H, Huang S, Zhu P. Resveratrol protects against TNF-α-induced injury in human umbilical endothelial cells through promoting sirtuin-1-induced repression of NF-KB and p38 MAPK. PLoS One. 2016;11(1):e0147034.
28. Deng HF, Wang S, Li L, Zhou Q, Guo WB, Wang XL, et al. Puerarin prevents vascular endothelial injury through suppression of NF-κB activation in LPS-challenged human umbilical vein endothelial cells. Biomed Pharmacother. 2018;104:261-7.
29. Luo E, Wang D, Yan G, Qiao Y, Zhu B, Liu B, et al. The NF-κB/miR-425-5p/MCT4 axis: a novel insight into diabetes-induced endothelial dysfunction. Mol Cell Endocrinol. 2020;500:110641.
30. Zhang Q, Lenardo MJ, Baltimore D. 30 years of NF-κB: a blossoming of relevance to human pathobiology. Cell. 2017;168(1-2):37-57.
31. Oeckinghaus A, Hayden MS, Ghosh S. Crosstalk in NF-κB signaling pathways. Nat Immunol. 2011;12(8):695-708.
32. Wang Z, Zhao H, Tian L, Zhao M, Xiao Y, Liu S, et al. Quantitative analysis and differential evaluation of Radix Bupleuri cultivated in different regions based on HPLC-MS and GC-MS combined with multivariate statistical analysis. Molecules. 2022;27(15):4830.
33. Yuan B, Yang R, Ma Y, Zhou S, Zhang X, Liu Y. A systematic review of the active saikosaponins and extracts isolated from Radix Bupleuri and their applications. Pharm Biol. 2017;55(1):620-35.

 https://doi.org/10.3831/KPI.2025.28.1.57